"This is the pre-peer reviewed version of the following article: - A highly fluorinated iridium complex as a blue-green emitting component for white electroluminescence- Synthetic Metals 227 (2017) 148-155, which has been published in final form at https://doi.org/10.1016/j.synthmet.2017.04.002.

A highly fluorinated iridium complex as a blue-green emitting component for white electroluminescence

R. Ragni,*[a] V. Maiorano,*[b] M. Pugliese,[b] A. Maggiore,[c] E. Orselli,[d,e] F. Babudri,[a] G. Gigli,[b,c] L. De Cola[f] and G. M. Farinola[a]

a. Dipartimento di Chimica, Università degli Studi di Bari ''Aldo Moro'', via Orabona 4, 70126 Bari, Italy. E-mail: roberta.ragni@uniba.it.

b. CNR NANOTEC, Institute of Nanotechnology, Campus Ecotekne, University of Salento, Via Monteroni, 73100 Lecce, Italy. E-mail: vincenzo.maiorano@nanotec.cnr.it

c. Department of Mathematics and Physics "Ennio De Giorgi", University of Salento, Campus Universitario, via Monteroni, 73100 Lecce, Italy.

d. Physikalisches Institut, Westfälische Wilhelms-Universität Münster Mendelstrasse 7, 48149 Münster, Germany.

e. Covestro Deutschland AG, Chempark Leverkusen, D-51365 Leverkusen, Germany

f. Institut de Science et d'Ingénierie Supramoléculaires, Université de Strasbourg & CNRS, 8 allée Gaspard Monge, 67083 Strasbourg Cedex, France.

Abstract

A novel perfluorinated heteroleptic iridium complex, namely iridium(III)bis[2-(2,5,2',3',4',5',6'-heptafluoro-biphenyl-4-yl)-pyridinato-N,C2'][3-(pentafluorophenyl)-pyridin-2-yl-1,2,4-triazolate] (Ir-F19), has been synthesized and characterized both in solution and in the solid state. The compound displays blue-green photoluminescence, with emission peaks at 480 and 512 nm and 68% quantum yield, in degassed acetonitrile solution. The use of this phosphor in blue and white organic light emitting devices (WOLEDs) has been investigated. Current efficiency of 8.3 cd/A at 100 cd/m^2 has been recorded for the blue emitting device whereas white electroluminescence with good color rendering index (CRI=76) and CIE coordinates (0.43,0.42) have been observed for a WOLED made of two stacked layers based on Ir-F19 and the commercial orange Ir(MDQ)$_2$(acac) [bis(2-methyldibenzo[f,h]quinoxaline)(acetylacetonate)iridium(III)]. WOLED luminous efficiency of 10.5 cd/A at 100 cd/m^2, almost constant (10.1 cd/A) up to 1000 cd/m^2, indicates that Ir-F19 is a promising blue-green emitting component for white electroluminescence.

Keywords

Iridium complexes, fluorinated emitters, white electroluminescence, OLEDs.

1. Introduction

Heteroleptic iridium complexes [(C^N)$_2$Ir(LX)] bearing two 2-arylpyridinate (C^N) and one ancillary (LX) ligands are among the most promising phosphorescent emitters for optoelectronics and lighting applications.[1-4] They combine high quantum efficiencies, due to the strong spin-orbit coupling of heavy metal phosphors,[5,6] with easier synthetic accessibility versus their homoleptic

$Ir(C\hat{}N)_3$ counterparts,[7,8] as well as tunable emission wavelength by proper chemical design and functionalization of the organic ligands.[9-12] In particular, fluorinated iridium complexes attract attention as effective and not so numerous blue phosphors for fabrication of blue and white organic light emitting devices (OLEDs). In fact, fluorination is a suitable functionalization to blue-shift light emission, to increase volatility favouring vapour deposition, to enhance electron mobility, and to prevent close packing that can cause electroluminescence self-quenching of molecular active materials in devices.[13-15]

White electroluminescence in OLEDs can result from simultaneous emission of three (red, green and blue) or two (most commonly blue and orange) emitting components blended in a single host material or confined in different stacked layers. An advantage of white OLED architectures based on emitters confined in different layers consists in (*i*) inhibition of complete energy transfer, which is a major issue in electroluminescence from blends, eventually leading to the emission from the sole low energy (orange/red) emitter, and (*ii*) good control of white colour emission by individually optimizing the thickness and the emitter concentration in each of the stacked layer. Nevertheless, stacked white OLEDs manufacture is more complex than solution processing of blends of different emitters. On this ground, the use of two layers with complementary (blue and orange) emission colours is desirable versus stacking three layers emitting fundamental colours. Examples of WOLEDs based on vacuum deposited stacked layers of two iridium complexes emitting complementary colours (blue and orange) are quite limited. For example, white electroluminescence was obtained by Yu *et al.*, with a maximum current efficiency of 11.08 cd/A, using the sky-blue iridium(III)[bis(4,6-difluorophenyl)-pyridinato-N,$C^{2'}$]picolinate complex (FIrpic) and the yellow complex bis[2-(4-tertbutylphenyl)benzothiazolato-N,$C^{2'}$]iridium(acetylacetonate) in a two stacked layer device architecture.[16] Deng *et al.* also used the same approach to fabricate a white OLED with FIrpic and a tailored orange diphenylphosphorylpyridine-iridium complex, achieving an efficiency of 23.9 cd/A with CIE coordinates (0.29, 0.43).[17] However, apart from few exceptions, most devices based on two stacked emitting layers suffer from colour rendering index values (CRI<70) lower than those of three layer devices.[18] Moreover, their luminous efficiency generally rolls off by increasing brightness and current density, as a combined effect of field-induced quenching and triplet-triplet annihilation.[19,20] Among exceptions, high current efficiency of 54.8 cd/A at high brightness (5000 cd/m^2) were reported by Wang *et al.* for a device based on two stacked emitting layers of FIrpic and an orange iridium complex with trifluoromethyl substituted 2-phenylbenzothiazole ligands.[21] Sasabe *et al.* recorded a CRI of 73 for a two-color WOLED using a blue emitting cyclometalated carbene iridium complex and the yellow emitter bis(2-phenylbenzothiazolato)(acetylacetonate)iridium(III).[22]

Here we report the synthesis and the photophysical characterization of a new heteroleptic iridium complex (Ir-F19 in Fig. 1), bearing highly fluorinated cyclometalating ligands and acting as an efficient blue/green phosphor. A two-color based stacked WOLED with CRI of 76, CIE coordinates

(0.43,0.42) and 10.5 cd/A luminous efficiency at 100 cd/m^2, almost constant (10.1 cd/A) up to 1000 cd/m^2, has been constructed using Ir-F19 as the blue component in combination with the commercial orange emitter bis(2-methyldibenzo[f,h]quinoxaline)(acetylacetonate)iridium [Ir(MDQ)$_2$(acac), Fig.1].

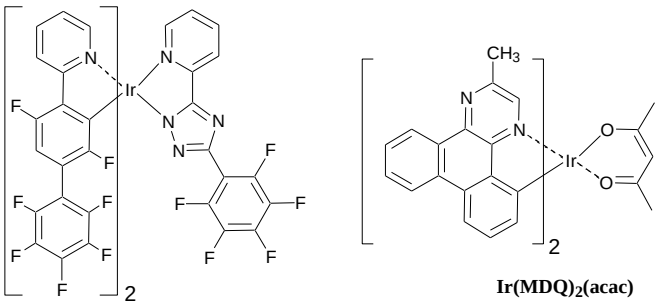

Fig. 1 Chemical structures of Ir-F19 and Ir(MDQ)$_2$(acac) emitters

2. Experimental

2.1 Synthesis of Ir-F19

All reactions were carried out under a nitrogen atmosphere and using dry solvents, unless otherwise stated. Tetrahydrofuran, 1,4-dioxane and toluene were distilled immediately prior to use from sodium and benzophenone. All starting materials and catalysts were purchased at the highest commercial purity degree from Sigma Aldrich and used without further purification. The ancillary ligand **4** was prepared according to the literature.[23] Column chromatography was performed on silica gel 60, (40–63 mm) from Merck. Merck silica gel 60 F254 aluminum sheets were also used for analytical TLC. All new compounds were characterized by high resolution mass spectrometry and FT-IR, ^{1}H-, ^{13}C-, and ^{19}F-NMR spectroscopies. Mass spectrometry was carried out by a Shimadzu high performance liquid chromatography-ion trap-time of flight mass spectrometer (LCMS-IT-TOF). FT-IR spectra were recorded using a Perkin–Elmer Spectrum BX spectrophotometer with dry KBr pellets. ^{1}H-, ^{13}C- and ^{19}F-NMR spectra were recorded at 400, 100 and 376 MHz, respectively, by using a Varian Inova 400 and a Agilent Technologies 500/54 Premium Shielded spectrometer. The residual proton signals of $CDCl_3$ and CD_2Cl_2 at δ=7.26 and 5.36 ppm, respectively, were used as references for the ^{1}H NMR spectra, whereas the signals of $CDCl_3$ and CD_2Cl_2 at δ=77.0 and 53.8 ppm were used as references for the ^{13}C NMR spectra. The ^{19}F signal of trichlorofluoromethane was used as the internal standard at δ=0.0 ppm for the ^{19}F NMR spectra. Melting points were determined on a Stuart Scientific Apparatus SMP3 (UK).

2.1.1 Synthesis of 2-(4-bromo-2,5-difluoro-phenyl)-pyridine (1)

In a 100 mL three-necked round bottom flask, the catalyst Pd(AsPh$_3$)$_4$ was prepared *in situ* by suspending Pd$_2$(dba)$_3$ (0.400 g, 0.44 mmol) and triphenylarsine (1.080 g, 3.52 mmol) in toluene (45

ml) at room temperature, under a nitrogen atmosphere. After few minutes, 1,4-dibromo-2,5-difluorobenzene (4.000 g, 14.70 mmol) and a solution of 2-(tributylstannyl)pyridine (5.960 g, 16.20 mmol) in toluene (15 ml) were added in sequence, under a nitrogen atmosphere. The resulting reaction mixture was stirred for 12 hours at 90 °C. After cooling to room temperature, the solvent was removed at reduced pressure. Water (30 ml) was added and the crude product was extracted three times with diethyl ether (30 ml). The organic extracts were combined and concentrated to a final volume of 30 ml by vacuum distillation. Organotin by-products were precipitated by addition of a solution of KF (4 g) in distilled water (10 ml) and filtered off. The organic solution was dried with anhydrous Na_2SO_4 and the solvent was removed in vacuo. The product **1** was isolated in 45% yield by column chromatography over silica gel, using a mixture of hexane and ethyl acetate (volume ratio 95:5) as the eluent. Mp: 87-88 °C. ^{1}H NMR (400 MHz, $CDCl_3$): δ 7.29 (ddd, *J*=7.3, 4.8, 1.3 Hz, 1H), 7.39 (dd, $^3J_{HF}$=10.0, $^4J_{HF}$=5.5 Hz, 1H), 7.77 (td, *J*=7.3, 1.8 Hz, 1H), 7.79-7.83 (m, 1H), 7.88 (dd, $^3J_{HF}$=9.3, $^4J_{HF}$=6.7 Hz, 1H), 8.71 (ddd, *J*=4.8, 1.8, 1.0 Hz, 1H) ppm. ^{13}C NMR (400 MHz, $CDCl_3$): δ 109.50 (dd, $^2J_{CF}$=23.9, $^3J_{CF}$=10.2 Hz), 117.51 (dd, $^2J_{CF}$=26.1, $^3J_{CF}$ ~ 3.9 Hz), 121.05 (d, $^2J_{CF}$=28.7 Hz), 123.15, 124.28 (d, $^4J_{CF}$=11.0 Hz), 127.95 (dd, $^2J_{CF}$=13.7, $^3J_{CF}$=6.7 Hz), 136.65, 149.88, 151.22 (dd, $^3J_{CF}$=3.3, $^4J_{CF}$=1.4 Hz), 155.88 (dd, $^1J_{CF}$=243.9, $^4J_{CF}$=2.7 Hz), 155.91 (dd, $^1J_{CF}$=250.1, $^4J_{CF}$=2.7 Hz) ppm. ^{19}F NMR (500 MHz, $CDCl_3$): δ -121.12÷-121.02 (m, 1F), -113.75÷-113.63 (m, 1F) ppm. FTIR (KBr): ν=3029, 1767, 1620, 1593, 1572, 1490, 1463, 1439, 1390, 1290, 1174, 1159, 1070, 993, 891, 797, 781, 741, 723, 697, 619 cm^{-1}. HRMS: $[M+H]^+$ *m/z* calcd 269.9724, found 269.9701.

2.1.2 Synthesis of 2-(2,5,2',3',4',5',6'-heptafluoro-biphenyl-4-yl)-pyridine (2)

In a 250 mL three-necked round bottom flask, magnesium powder (0.600 g, 24.7 mmol) was suspended in dry THF (35 ml) and activated by adding one little grain of iodine, under a nitrogen atmosphere. Then, the suspension was heated to reflux and a solution of bromopentafluorobenzene (5.080 g, 20.6 mmol) in dry THF (5 ml) was added dropwise by a dropping funnel. The reaction mixture was stirred at 90 °C for two hours and the complete conversion of bromopentafluorobenzene into pentafluorophenyl magnesium bromide was confirmed via GC/MS analysis observing the presence of deuteropentafluorobenzene after quenching a small sample of the mixture with deuterium oxide. After cooling to room temperature, sequential additions of CuBr (5.900 g, 41.1 mmol), dry 1,4-dioxane (20 ml) and a solution of **1** (1.390 g, 5.14 mmol) in dry toluene (40 ml) were respectively carried out, under a nitrogen atmosphere, waiting one hour between each addition. Then, the system was heated overnight at 90 °C. The complete disappearance of **1** was confirmed after 12 hours via TLC. After cooling to room temperature, the organic solvents were distilled at reduced pressure and the crude product dissolved into diethylether (50 ml). The solution was filtered to remove inorganic salts, washed with water (30 ml) and then dried with anhydrous sodium sulphate. After the distillation of the solvent at reduced pressure, the organic ligand **2** was isolated in 84% yield by column chromatography, using a mixture of hexane and dichloromethane (volume ratio 30:70) as the eluent.

Yield: 84%. Mp: 149-150 °C. ^{1}H NMR (400 MHz, $CDCl_3$): δ 7.20 (dd, $^{3}J_{HF}$ = 10.5, $^{4}J_{HF}$ = 5.5 Hz, 1H), 7.34 (ddd, *J* = 7.5, 4.8, 1.2 Hz, 1H), 7.82 (td, *J* = 7.6, 1.8 Hz, 1H), 7.87-7.92 (m, 1H), 7.97 (dd, $^{3}J_{HF}$ = 10.1, $^{4}J_{HF}$ = 6.4 Hz, 1H), 8.76 (ddd, *J* = 4.8, 1.8, 1.0 Hz, 1H) ppm. ^{13}C NMR (500 MHz, $CDCl_3$): δ 108.51-109.23 (m), 115.19-115.65 (m), 117.89 (dd, $^{2}J_{CF}$ = 26.0, $^{3}J_{CF}$ = 3.6 Hz), 129.29 (d, $^{2}J_{CF}$ = 27.5 Hz), 123.38, 124.51 (d, $^{4}J_{CF}$ = 10.8 Hz), 130.42 (dd, $^{2}J_{CF}$ = 13.7, $^{3}J_{CF}$ = 7.8 Hz), 136.70, 137.71 (dm, $^{1}J_{CF}$ ~ 256 Hz), 141.46 (dm, $^{1}J_{CF}$ ~ 256 Hz), 144.31 (dm, $^{1}J_{CF}$ ~ 251 Hz), 150.00, 151.22, 155.96 (dm, $^{1}J_{CF}$ ~ 248 Hz), 156.15 (dm, $^{1}J_{CF}$ ~ 248 Hz) ppm. ^{19}F NMR (500 MHz, $CDCl_3$): δ -161.97 (td, $^{3}J_{FF}$ = 21.0 Hz, $^{4}J_{FF}$ = 7.0 Hz, 2F), -153.34 (tl, $^{3}J_{FF}$~21.0 Hz, 1F), -140.32÷-140.18 (m, 2F), -122.29÷-122.14 (m, 1F), -118.40÷-118.22 (m, 1F) ppm. FTIR (KBr): ν = 3096, 3059, 1653, 1589, 1530, 1489, 1465, 1440, 1402, 1178, 1071, 988, 887, 844, 794, 769, 747, 723, 615 cm^{-1}. HRMS: $[M+H]^+$ *m/z* calcd 358.0461, found 358.0436.

2.1.3 Synthesis of tetrakis[2-(2,5,2',3',4',5',6'-heptafluoro-biphenyl-4-yl)-pyridinato-N,C2'](μ-dichloro)diiridium (3)

The ligand **2** (1.400 g, 3.9 mmol) and $IrCl_3 \cdot 3H_2O$ (0.555 g, 1.6 mmol) were suspended in 2-ethoxyethanol (21 ml) and water (7 ml) under a nitrogen atmosphere. The reaction mixture was refluxed overnight and then cooled to room temperature. Water (20 ml) was added and the crude product was filtered on a büchner funnel as a yellow solid. The dimer complex **3** was directly purified as a solid on filter by washing it with hexane (100 ml) to remove the soluble residual ligand **2**. Yield: 70%. ^{1}H NMR (400 MHz, $CDCl_3$): δ 6.66 (dd, $^{3}J_{HF}$ = 11.4, $^{4}J_{HF}$ = 4.8 Hz, 4H), 6.72 (td, *J* = 7.2, 1.2 Hz, 4H), 7.82 (td, *J* = 7.9, 1.4 Hz, 4H), 8.38 (bd, *J* = 8.8 Hz, 4H), 9.01 (d, *J* = 5.8 Hz, 4H) ppm. ^{13}C NMR (500 MHz, CD_2Cl_2): δ 109.90-110.34 (m), 113.45 (d, $^{2}J_{CF}$ = 27.9 Hz), 115.01 (dd, $^{2}J_{CF}$=25.3, $^{3}J_{CF}$=11.0 Hz), 123.72, 124.19 (d, $^{2}J_{CF}$ = 21.5 Hz), 126.31 (d, $^{2}J_{CF}$ = 36.4 Hz), 137.68 (dd, $^{2}J_{CF}$ = 14.4, $^{3}J_{CF}$ =6.7 Hz), 138.06 (dm, $^{1}J_{CF}$ = 250.1 Hz), 138.23, 141.41 (dm, $^{1}J_{CF}$ = 259.3 Hz), 144.59 (dm, $^{1}J_{CF}$ = 249.2 Hz), 153.05, 156.03 (dm, $^{1}J_{CF}$ = 252.6 Hz), 161.25 (dm, $^{1}J_{CF}$ = 238.9 Hz), 165.28 (d, $^{3}J_{CF}$ = 7.1 Hz) ppm. ^{19}F NMR (500 MHz, CD_2Cl_2): -163.30÷-162.85 (m, 8F), -155.17 (tl, $^{3}J_{FF}$ = 20.7 Hz, 4F), -140.87 (bd, $^{3}J_{FF}$ = 22.3 Hz, 4F), -140.0÷-139.65 (m, 4F), -119.29 (dd, $^{3}J_{HF}$ = 11.4, $^{5}J_{FF}$ = 19.7 Hz, 4F), -111.50 ÷ -111.25 (m, 4F) ppm. FTIR (KBr): ν = 3091, 1652, 1607, 1569, 1558, 1522, 1495, 1463, 1417, 1382, 1327, 1302, 1185, 1078, 989, 824, 786, 758, 730 cm^{-1}. HRMS: $[M/2-Cl]^+$ *m/z* calcd 905.0246, found 905.0279.

2.1.4 Synthesis of iridium(III)bis[2-(2,5,2',3',4',5',6'-heptafluoro-biphenyl-4-yl)-pyridinato-N,C^2'][3-(pentafluoro-phenyl)-pyridin-2-yl-1,2,4-triazolate] (Ir-F19)*

The dimer complex **3** (0.600 g, 0.32 mmol) and the ligand **4** (0.220 g, 0.70 mmol) were dissolved under a nitrogen atmosphere in previously degassed dichloromethane (15 ml) and ethanol (15 ml). The solution was stirred for 24 h at 60 °C under a nitrogen atmosphere. After cooling to room temperature, the reaction mixture was diluted with water (15 ml) and the crude product was extracted three times with dichloromethane (3x10 ml). The organic extracts were dried with anhydrous Na_2SO_4. Then, the solvent was distilled under reduced pressure and Ir-F19 was isolated by column

chromatography over silica gel with a mixture of dichloromethane/hexane/acetone (60:35:5) as the eluent.

Yield: 67%. ^{1}H NMR (400 MHz, CD_2Cl_2): δ 6.77 (dd, $^{3}J_{HF}$ = 11.6, $^{4}J_{HF}$ = 5.0 Hz, 1H), 6.86 (dd, $^{3}J_{HF}$ = 11.6, $^{4}J_{HF}$ = 5.0 Hz, 1H), 6.90-6.99 (m, 2H), 7.28 (ddd, *J* = 7.2, 5.6, 1.3 Hz, 1H), 7.63 (bd, *J* =5.0 Hz, 1H), 7.68-7.75 (m, 3H), 7.90 (bd, *J* = 5.4 Hz, 1H), 7.97 (td, *J* = 7.7, 1.4 Hz, 1H), 8.25-8.33 (m, 3H) ppm. ^{13}C NMR (400 MHz, CD_2Cl_2): 110.02÷110.26 (m), 110.50÷110.76 (m), 113.04 (d, $^{2}J_{CF}$=29.2 Hz), 113.86 (d, $^{2}J_{CF}$ = 27.9 Hz), 114.95÷115.36 (m), 115.70÷116.08 (m), 122.59, 123.50, 123.9, 124.19 (d, $^{4}J_{CF}$ = 3.1 Hz), 124.36 (d, $^{4}J_{CF}$ = 3.4 Hz), 126.07, 130.21, 131.14, 131.46, 134.47, 136.17, 136.51, 137.14-137.37 (m), 137.54 (dd, $^{2}J_{CF}$ = 16.0, $^{3}J_{CF}$ = 6.0 Hz) 138.22 (dm, $^{1}J_{CF}$ = 248.0 Hz), 138.43, 138.67, 140.15, 141.47 (bd, $^{1}J_{CF}$ = 247.4 Hz), 144.82 (bd, $^{1}J_{CF}$ = 248.5 Hz), 145.73 (bd, $^{1}J_{CF}$ = 254.6 Hz), 149.86, 149.97, 151.28, 151.86, 153.93, 156.85 (d, $^{1}J_{CF}$ = 253.5 Hz), 157.30 (d, $^{1}J_{CF}$ = 253.6 Hz), 161.91 (dm, $^{1}J_{CF}$ = 236.1 Hz), 162.24 (dm, $^{1}J_{CF}$ = 235.3 Hz), 164.12, 165.11 (d, $^{3}J_{CF}$ = 7.0 Hz), 165.44 (d, $^{3}J_{CF}$ = 7.0 Hz), 165.83 ppm ppm. ^{19}F NMR (500 MHz, CD_2Cl_2): -163.70 (m, 2F), -163.38÷-162.92 (m, 3F), -162.80÷-162.52 (m, 1F), -155.96 (t, $^{3}J_{FF}$= 20.7 Hz, 1F), -155.44 (t, $^{3}J_{FF}$= 20.7 Hz, 1F), -155.02 (t, $^{3}J_{FF}$= 20.7 Hz, 1F), -140.59÷-140.23 (m, 5F), -140.06÷-139.69 (m, 1F), -119.61÷-119.44 (m, 1F), -119.16÷-119.01 (m, 1F), -110.78÷-110.61 (m, 1F), -109.28÷-109.10 (m, 1F) ppm. FTIR (KBr): ν = 3064, 1652, 1613, 1569, 1522, 1498, 1478, 1461, 1441, 1416, 1381, 1326, 1299, 1184, 1076, 990, 842, 822, 788, 758, 729 cm^{-1}. HRMS: $[M+H]^+$ *m/z* calcd 1217.0681, found 1217.0695.

2.2 Photophysical characterization in solution

UV-Vis absorption spectra were recorded on a Hewlett-Packard diode array 84533 spectrophotometer. Recording of the emission spectra was done with a SPEX Fluorolog spectrofluorometer. Low temperature (77 K) emission spectra for glasses and solid state samples were recorded in 5 mm diameter quartz tubes which were placed in a liquid nitrogen Dewar equipped with quartz walls. The emission spectra were corrected for monochromator and photomultiplier efficiency and for xenon lamp stability. Sample and standard solutions were degassed with at least three freeze-pump-thaw cycles. All solvents were spectrometric grade and all solutions were filtered through a 0.2 μm syringe filter before measurement. Emission quantum yields were measured by the method of Demas and Crosby,[24] using quinine disulfate in 0.5 M sulfuric acid as the standard (Φ=0.546). Lifetimes were determined using a Coherent Infinity Nd:YAG-XPO laser (1 ns pulses FWHM) and a Hamamatsu C5680-21 streak camera equipped with a Hamamatsu M5677 Low-Speed Single-Sweep Unit.

2.3 Cyclic voltammetry

CV was performed by a Voltalab 40 system from Radiometer Analytical, which consists of a PGZ301 potentiostat and Voltamaster 4 software.[25] The working and counter electrodes were a Pt-disc and a Pt wire, respectively, and Ag wire was used as the pseudoreference electrode. All glassware was dried prior to use. The dry electrolyte tetrabutylammonium hexafluorophosphate (>99.0% purity), the analyte and ferrocene ($FeCp_2$ used as the reference) were dried and degassed in

a Schlenk flask at high temperature and reduced pressure to eliminate any moisture and oxygen. The flask was then evacuated and filled three times with N_2. Acetonitrile, freshly distilled from P_2O_5, was added directly to the sealed Schlenk flask by a syringe. The solution was sonicated and degassed for ten minutes with a gentle stream of nitrogen; then, it was injected into the electrochemical cell and, after the introduction of electrodes, measurements were performed under a nitrogen atmosphere.

2.4 Photoluminescence measurements on thin films

Emission spectra of films were recorded with an Edinburgh FLS980 spectrometer equipped with a peltier-cooled Hamamatsu R928 photomultiplier tube (PMT, 185-850 nm). An Edinburgh Xe900 450 W Xenon arc lamp was used as the exciting light source. Emission lifetimes in the ns-µs range were determined with the single photon counting technique by means of the same Edinburgh FLS980 spectrometer using the above-mentioned PMT as the detector and a laser diode as the excitation source (1 MHz, λ_{exc} = 407 nm, 200 ps time resolution after deconvolution). Analysis of the luminescence decay profiles versus time was accomplished with the Decay Analysis Software provided by the manufacturer. For solid samples, emission quantum yields were calculated following the procedure described by De Mello *et al.*,[26] using corrected emission spectra obtained by an apparatus based on a barium sulphate coated integrating sphere (4 inches), a 450W Xe lamp (λ_{exc} tunable by a monochromator supplied with the instrument) and a R928 photomultiplier detector tube. Experimental uncertainties were estimated as ± 8% for lifetime determinations, ± 20% for emission quantum yields, ± 2 nm and ± 5 nm for absorption and emission peaks, respectively.

2.5 OLEDs fabrication and characterization

OLEDs were fabricated by high vacuum thermal evaporation in a Kurt J. Lesker multiple high vacuum chamber system. The electrical-optical characteristics of devices were measured under vacuum, using an Optronics OL770 spectrometer coupled by an optical fiber to the OL610 telescope unit for the luminance measurements. The whole system was National Institute of Standards and Technology (NIST) calibrated using a standard lamp and was directly connected by RS232 cable to a Keithley 2420 current-voltage source meter.

3. Results and discussion

3.1 Synthesis of Ir-F19

The synthesis of Ir-F19 requires the preliminary preparation of the cyclometalating ligands **2** and **4**, the latter being already reported in the literature.[23] **2** was obtained by the Stille cross-coupling reaction of 2-(tributylstannyl)pyridine with 1,4-dibromo-2,5-difluorobenzene in the presence of toluene as the solvent and $Pd(AsPh_3)_4$ as the catalyst prepared *in situ* (Scheme 1). The resulting arylbromide **1** was isolated in 45% yield and used in a Ullmann type reaction [27,28] with pentafluorophenyl copper, obtained *in situ* by the metalation reaction of bromopentafluorobenzene with magnesium powder and transmetalation of the resulting Grignard intermediate with cuprous bromide (Scheme 1).

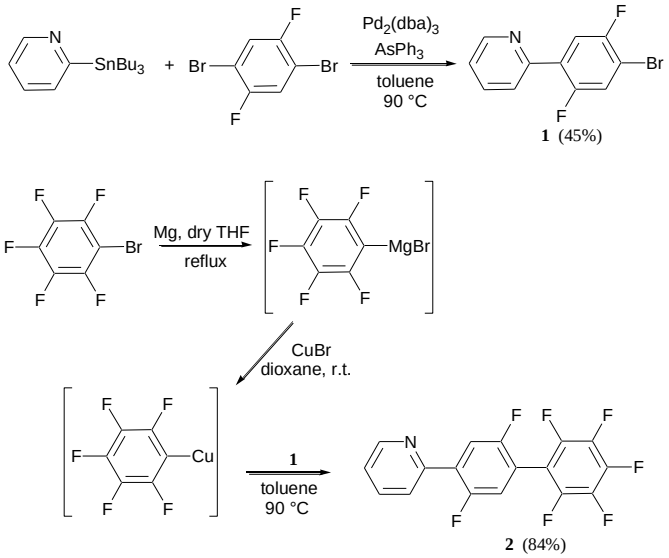

Scheme 1. Synthesis of ligand **2**

Compound **2** was obtained as a white solid in 84% yield and used as the cyclometalating ligand in the complexation reaction with $IrCl_3 \cdot 3H_2O$ (Scheme 2).[29,30] The resulting dimer complex **3** was reacted with the ligand **4** in a deaerated mixture of dichloromethane and ethanol, yielding 67% of Ir-F19 as a pale yellow solid (Scheme 2).

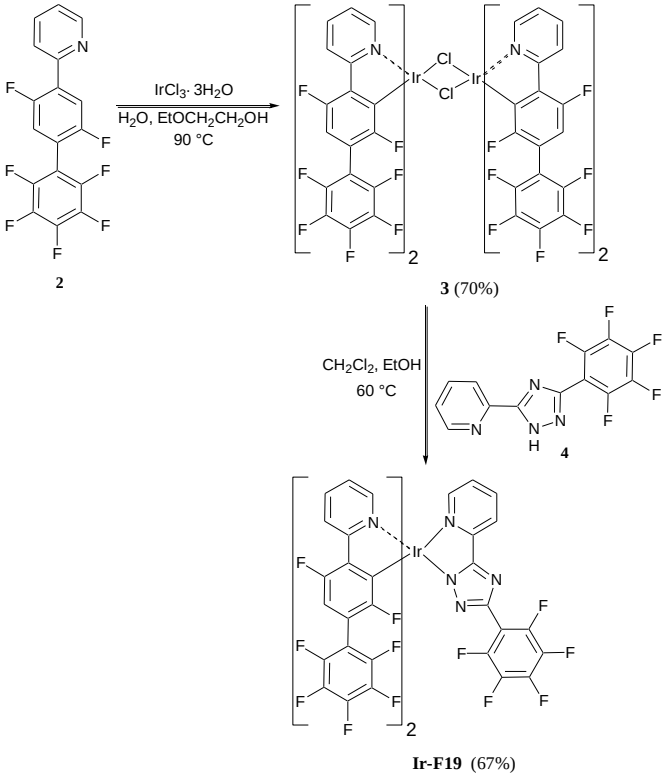

Scheme 2. Synthesis of Ir-F19

3.2 Photophysical and electrochemical properties of Ir-F19 in solution

Absorption and emission spectra of Ir-F19 in acetonitrile solution at room temperature are reported in Fig. 2 and all data regarding the characterization of this complex in solution are summarized in Table 1. Ir-F19 absorbs light in the UV and visible regions: the intense band at high energies (<350 nm) can be assigned to singlet $^1(\pi–\pi^*)$ transitions localized on the coordinated ligands. The highest energy absorption is due to transitions centred on the phenylpyridine ligands, and the shoulder at ~320 nm is attributed to transitions centred on the triazole ligand. The weak absorption in the visible region can be assigned mainly to singlet and triplet metal to ligand charge transfer (MLCT) transitions similar to those found for other iridium phenylpyridine-pyridinetriazole type complexes.[23]

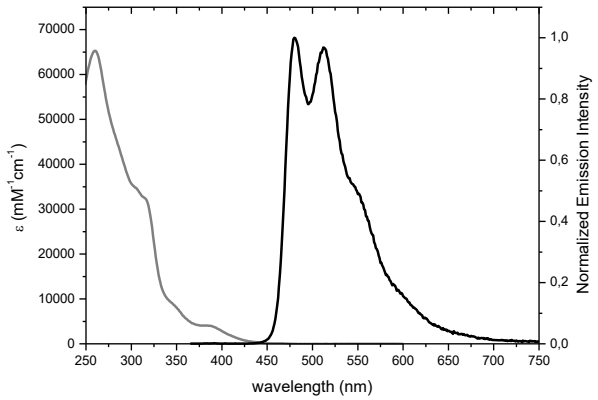

Figure 2. Absorption (red) and emission (black) spectra of Ir-F19 in acetonitrile (λ_{exc} =350 nm)

Ir-F19 photoluminescence spectrum at room temperature in acetonitrile solution (Figure 2) exhibits a maximum in the blue region at 480 nm and vibrational progression in the green spectral regions, at 512 nm and a shoulder at 550 nm. The nature of the excited state is attributed to a ligand centred (LC) with admixed MLCT states. Indeed this luminescent mixed state is characterized by a rather long excited state lifetime and by a moderate variation of its energy upon freezing the solution. In fact, the emission in rigid matrix, as butyronitrile glass, exhibits only a few nanometers blue shift (473 nm) and an elongation of the excited state lifetime to 6.5 μs (see table 1). The typical rigidochromic shift toward higher energies, corroborate the assignment of the partial ^{3}MLCT character to the excited state together with a ^{3}LC character as suggested by the structure of both emission spectra at 298 and 77 K (see also SI, S15).

Emission quantum yield in degassed solution is relatively high (68%), and its oxygen sensitivity (4.7% in air equilibrated conditions) is a confirmation of the triplet character of photoluminescence (Table 1). A significant enhancement of the excited-state lifetime in degassed versus air equilibrated acetonitrile solution was observed as well (5.8 μs *vs* 410 ns, Table 1).

Electrochemistry of the complex was investigated in acetonitrile solution using tetrabutylammonium hexafluorophosphate as the supporting electrolyte. At a scan rate of 100 mV/s, reversible oxidation and irreversible reduction waves were recorded by cyclic voltammetry, at +1.13 and at about -2.14 V versus

$FeCp_2^+/FeCp_2$, respectively. The oxidation mainly occurs on the phenyl ring of the ligand with a contribution of the iridium ion. The electron-withdrawing character of the fluorinated substituents lowers the HOMO and therefore the oxidation potential is more positive than that of the phenylpyridine complex analogues.

Table 1. Photophysical and electrochemical characterization of Ir-F19 in solution

Absorption [a]		Emission, 298 K					Emission, 77 K		Redox Potential (V) [c]	
(nm)	ε ($M^{-1}cm^{-1}$)	λ_{max} (nm) [a]	Φ^a	Φ^b	τ^a (μs)	τ^b (μs)	λ_{max} (nm) [c]	τ^a (μs)	$E_{1/2}^{ox}$	$E_{1/2}^{red}$
260	65300	480, 512	0.68	0.047	0.41	5.8	473, 507, 545	6.5	1.13	-2.14
317	31980									
347	8670									
385	4036									

[a] In air equilibrated acetonitrile. [b] In deoxygenated acetonitrile. [C] In butyronitrile glass.

3.3 Solid state photophysical characterization of Ir-F19

The photophysical properties of Ir-F19 were also analysed in neat film and in a blend with PMMA matrix (Ir-F19 weight ratio 0.1%) with the aim to compare light absorption of the complex in both neat and diluted solid matrix, and to evaluate the presence of aggregated absorbing states in the neat film. As shown in Fig. 3a, the UV-Vis absorption spectrum profile is very similar, for both films, to that recorded in solution. This means that no aggregate absorbing states formation is observed.

Two peaks are evident in the emission profile of the 0.1% Ir-F19:PMMA film (480 and 510 nm, respectively, Fig. 3b), whereas, in the neat film, the optical features and particularly the first peak are sensibly reduced in intensity. This effect can be attributed to the increased intermolecular interactions that favour the overlapping of many vibrational modes.[31] Moreover, we excluded the occurrence of self-absorption phenomena since no overlap between the absorption and emission spectra of the complex are observed. Finally, excitation spectra recorded at 500 nm (Fig. 3c), are in agreement with the absorption profiles, and again the change in ratio of the two bands can be assigned to the packing of the molecules. The PL lifetime is drastically reduced in the neat film compared to the blend (240 ns *vs* 4300 ns). This can be ascribed to the well-known self-quenching phenomena characteristic of octahedral Ir (III) complexes in the solid state.[19]

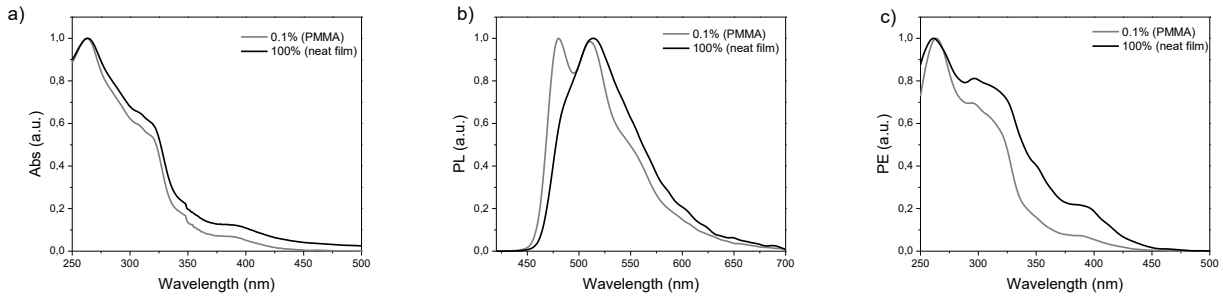

Figure. 3 Photophysical characterization of **Ir-F19** thin films at different concentrations (0.1 wt% in PMMA and 100%-neat film): a) absorption; b) photoluminescence; c) photo-excitation spectra.

3.4 Device data

Blue and white light emitting devices were fabricated using Ir-F19 as the sole emitter or in combination of the commercially available orange $Ir(MDQ)_2(acac)$ phosphor. P-i-n technology was used in the fabrication of both devices, with p-doping and n-doping for hole and electron transporting layers respectively, to ensure a very low driving voltage while maintaining device's power efficiency and lifetime.[32] The devices' architectures shown in Figure 4 ensure a good confinement of holes and electrons in the emitting layers.

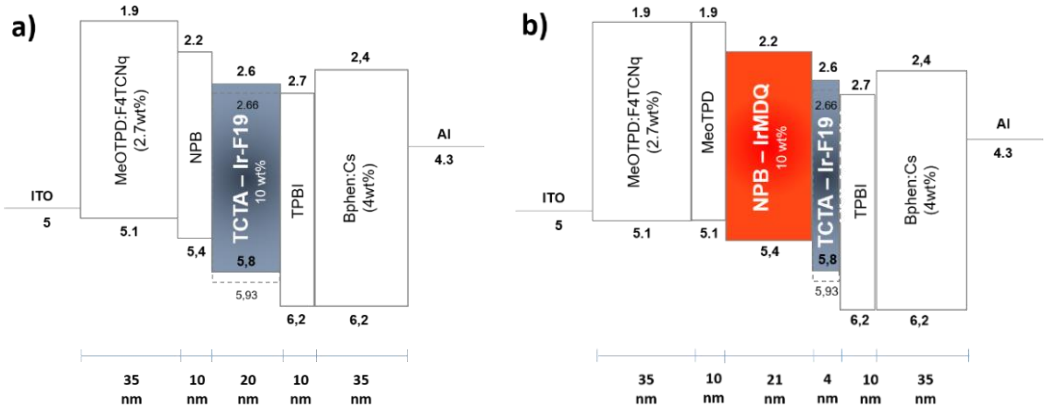

Figure. 4 a) Blue and b) white light emitting devices architectures

In particular, the blue OLED comprises a 20 nm thick emitting layer of Ir-F19 doped in (4,4',4"-tri(*N*-carbazolyl)-triphenylamine) (TCTA) host matrix. TCTA has high triplet energy and suppresses exciton quenching of blue triplet emitters thus improving the quantum efficiency of blue phosphorescent OLEDs.[33] 10% Ir-F19 weight ratio within TCTA was found to be the best value by determination of photoluminescence quantum yield of TCTA-IrF19 thin films, evaluated using increasing dopant concentration in the range from 5 wt% to 20 wt%. A 35 nm thin film of *N,N,N′,N′*-tetrakis(4-methoxyphenyl)benzidine (MeOTPD) doped with 2,3,5,6-tetrafluoro-7,7,8,8-tetracyanoquinodimethane (F4TCNQ) and a 35 nm film of 4,7-diphenyl-1,10-phenanthroline (Bphen) doped with Caesium were used as the hole and the electron transporting layers, respectively. Further 10 nm films of *N,N′*-di(1-naphthyl)-*N,N′*-diphenyl-(1,1′-biphenyl)-4,4′-diamine (NPB) and 2,2′,2"-(1,3,5-benzinetriyl)-tris(1-phenyl-1-H-benzimidazole) (TPBI) were used as the electron and hole blocking layers, respectively.

The electroluminescence spectrum (Fig. 5a) of the blue PHOLED (CIE x=0.13; y=0.27) is in line with the solid state Ir-F19 photoluminescence spectrum, showing two main peaks at 486 nm and 515 nm. Current efficiency of 8.3 cd/A at 3.3 mA/cm^2 (with a luminance of 270 cd/m^2) was observed for this device, rolling down in correspondence of high current density (Fig. 5d), due to exciton-quenching mechanisms.

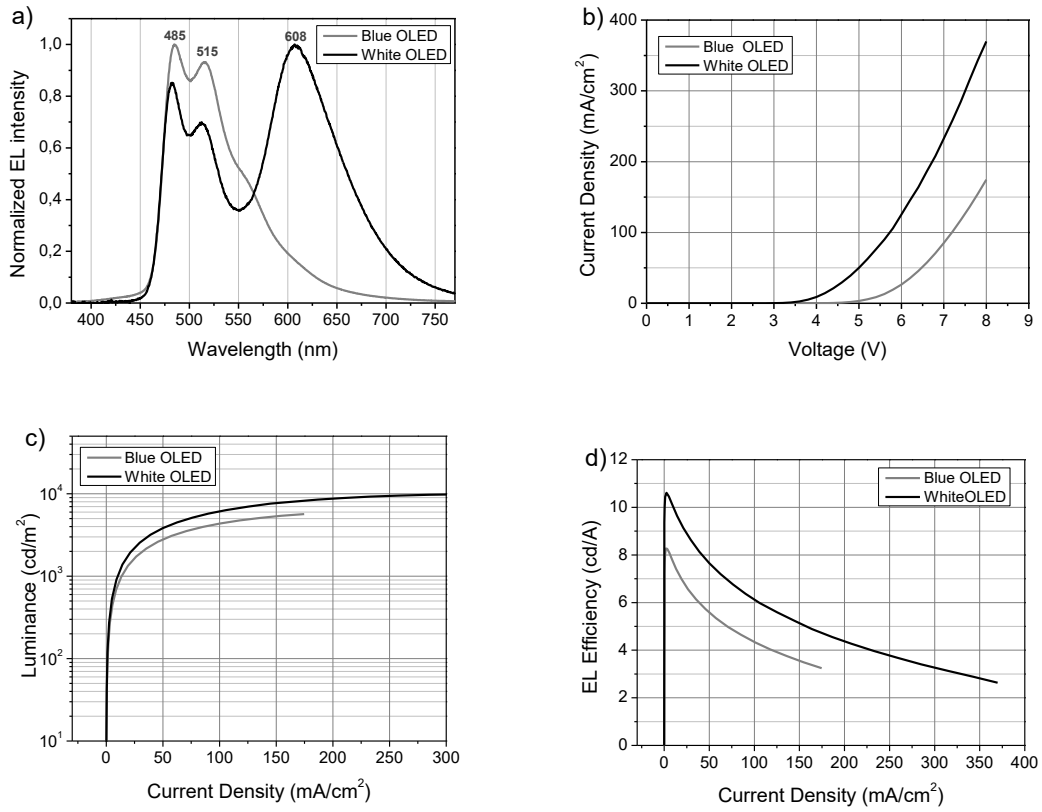

Figure. 5 Performances of blue and white OLEDs. a) Normalized electroluminescence spectra. b) Voltage-current density. c) Current density-Luminance and d) current density-efficiency characteristics.

The WOLED architecture is similar to that of the blue OLED. In this case, two stacked emitting layers were used consisting, respectively, of a 30 nm NPB film doped with the orange $Ir(MDQ)_2(acac)$ complex and a 4 nm TCTA layer doped with Ir-F19. A 10% wt concentration of the red phosphor was selected among various dopant concentrations as the best value by determination of the photoluminescence quantum yield. Moreover, in WOLED device, a 10 nm MeOTPD electron blocking layer was used between the hole transporting and the red emitting layers. The red and blue emitting layer thicknesses were optimized by an optical simulation software (ETFOS–Fluxim) in order to achieve the best CIE and CRI values.

The WOLED electroluminescence spectrum (Fig. 5a) shows a good balance of red and blue emission, leading to a device with colour rendering index (CRI) of 76 and CIE chromaticity coordinates (0.43, 0.42) (Fig. 6). Good current efficiency of 10.5 cd/A was also observed working at 100 cd/m^2, being almost constant (10.1 cd/A) up to 1000 cd/m^2. Moreover, the WOLED still keeps a current efficiency of 3 cd/A at 10000 cd/m^2, contrary to the efficiency close to zero generally observed in the literature for two color-based OLEDs under similar conditions.[18]

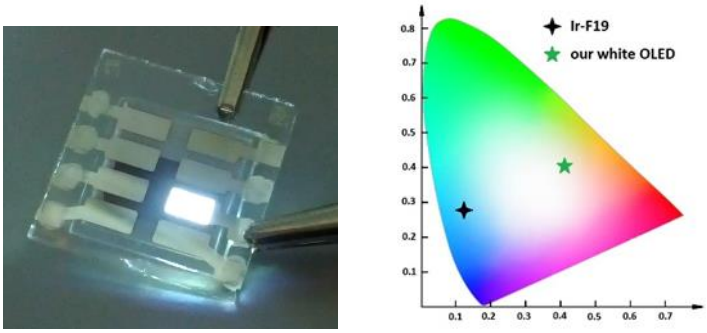

Figure. 6 An image of the white OLED (4.5V) and chromaticity coordinates in the CIE 1931 colour space of both blue and white Ir-F19 based devices.

4. Conclusions

In conclusion, we have synthesized and spectroscopically characterized a new highly fluorinated iridium complex, Ir-F19, with blue-green photoluminescence both in solution and in the solid state. Ir-F19 can be regarded as a promising phosphor for blue and white light emitting diodes. Although further studies are necessary to properly select devices' configuration and to optimize performances, our results show that Ir-F19 can be used to fabricate two emitting component white OLEDs with good colour rendering index (CRI 76) and efficiency of 10.1 cd/A at 1000 cd/m^2 that is still detectable at higher current densities (3 cd/A at 10000 cd/m^2).

5. Acknowledgements

This work was financed by Ministero dell'Istruzione dell'Università e della Ricerca (MIUR) and Università degli Studi di Bari (PON 02_00563_3316357 Molecular Nanotechnology for Health and Environment MAAT, PON03PE_00067_6 APULIA SPACE).

6. References

1 G. M. Farinola, R. Ragni, Electroluminescent materials for white organic light emitting diodes, Chem. Soc. Rev. 40 (2011) 3467-3482.

2 G. M. Farinola, R. Ragni, Organic emitters for solid state lighting, Journal of Solid State Lighting 2:9 **(**2015) 1-17.

3 K. T. Kamtekar, A. P. Monkman, M. R. Bryce, Recent Advances in White Organic Light-Emitting Materials and Devices (WOLEDs), Adv. Mater., 22 (2010) 572-582.

4 S. Reineke, F. Lindner, G. Schwartz, N. Seidler, K. Walzer, B. Lüssem, K. Leo, White organic light-emitting diodes with fluorescent tube efficiency, Nature 459 (2009) 234-238.

5 R. C. Evans, P. Douglas, C. J. Winscom, Coordination complexes exhibiting room-temperature phosphorescence: evaluation of their suitability as triplet emitters for light-emitting diodes, Coord. Chem. Rev. 250 (2006) 2093-2126.

6 H. Yersin, Highly Efficient OLEDs with Phosphorescent Materials, Wiley-VCH Verlag GmbH & Co. KGaA, Weinheim, 2008.

7 R. Ragni, E. A. Plummer, K. Brunner, J. W. Hofstraat, F. Babudri, G. M. Farinola, F. Naso, L. De Cola, Blue emitting iridium complexes: synthesis, photophysics and phosphorescent devices, J. Mater. Chem. 16 (2006) 1161-1170.

8 A. B. Tamayo, B. D. Alleyne, P. I. Djurovich, S. Lamansky, I. Tsyba, N. N. Ho, R. Bau, M. E. Thompson, Synthesis and Characterization of Facial and Meridional Tris-cyclometalated Iridium(III) Complexes, J. Am. Chem. Soc. 125 (2003) 7377-7387.

9 C. Ulbricht, B. Beyer, C. Friebe, A. Winter, U. S. Schubert, Recent Developments in the Application of Phosphorescent Iridium(III) Complex Systems, Adv. Mater. 21 (2009) 4418-4441.

10 R. Ragni, E. Orselli, G. S. Kottas, O. Hassan Omar, F. Babudri, A. Pedone, F. Naso, G. M. Farinola, L. De Cola, Iridium(III) complexes with Sulfonyl and Fluorine Substituents: Synthesis, Stereochemistry and Effect of Functionalisation on their Photophysical Properties, Chem. Eur. J., 15 (2009) 136-148.

11 W. Mróz, R. Ragni, F. Galeotti, E. Mesto, C. Botta, L. De Cola, G. M. Farinola, U. Giovanella, Influence of electronic and steric effects of substituted ligands coordinated to Ir(III) complexes on the solution processed OLED properties, J. Mater. Chem. C, 3 (2015) 7506-7512.

12 E. Mesto, F. Scordari, M. Lacalamita, L. De Cola, R. Ragni, G. M. Farinola, The correct assignment of stereochemistry in di-dichlorido-bis{bis[2-(5-benzylsulfonyl)-3-fluoro-2-(pyridin-2-yl)phenyl-2N,C1]iridium (III)} toluene monosolvate, Acta Cryst., C69 (2013) 480-482.

13 F. Babudri, G. M. Farinola, F. Naso, R. Ragni, Fluorinated organic materials for electronic and optoelectronic applications: the role of the fluorine atom, Chem. Commun. (2007) 1003.

14 B. Milián-Medina, S. Varghese, R. Ragni, H. Boerner, E. Ortí, G. M. Farinola, J. Gierschner, Excited-state switching by per-fluorination of para-oligophenylenes, J. Chem. Phys. 135 (2011) 124509-1-6.

15 C. Martinelli, U. Giovanella, A. Cardone, S. Destri, G. M. Farinola, A white emitting poly(phenylenevinylene), Polymer 55 (2014) 5125-5131.

16 J. Yu, W. Zhang, W. Wen, H. Lin, Y. Jiang, Film thickness influence of dual iridium complex ultrathin layers on the performance of nondoped white organic light-emitting diodes, Displays 32 (2011) 87-91.

17 L. Deng, T. Zhang, R. Wang, J. Li, Diphenylphosphorylpyridine-functionalized iridium complexes for high-efficiency monochromic and white organic light-emitting diodes, J. Mater. Chem. 22 (2012) 15910-15918.

18 S.-J. Su, E. Gonmori, H. Sasabe, J. Kido, Highly Efficient Organic Blue-and White-Light-Emitting Devices Having a Carrier- and Exciton-Confining Structure for Reduced Efficiency Roll-Off, Adv. Mater. 20 (2008) 4189-4194.

19 S. Reineke, K. Walzer, K. Leo, Triplet-exciton quenching in organic phosphorescent light-emitting diodes with Ir-based emitters, Phys. Rev. B 75 (2007) 125328.

20 M. A. Baldo, C. Adachi, S. R. Forrest, Transient analysis of organic electrophosphorescence. II. Transient analysis of triplet-triplet annihilation, Phys. Rev. B 62 (2000) 10967-10977.

21 R. Wang, D. Liu, H. Ren, T. Zhang, H. Yin, G. Liu, J. Li, Highly Efficient Orange and White Organic Light-Emitting Diodes Based on New Orange Iridium Complexes, *Adv. Mater.* 23 (2011) 2823-2827.

22 H. Sasabe, J.-i. Takamatsu, T. Motoyama, S. Watanabe, G. Wagenblast, N. Langer, O. Molt, E. Fuchs, C. Lennartz, J. Kido, High-Efficiency Blue and White Organic Light-Emitting Devices Incorporating a Blue Iridium Carbene Complex, Adv. Mater. 22 (2010) 5003-5007.

23 E. Orselli, G. S. Kottas, A. E. Konradsson, P. Coppo, R. Fröhlich, L. De Cola, A. van Dijken, M. Büchel, H. Börner, Blue-Emitting Iridium Complexes with Substituted 1,2,4-Triazole Ligands: Synthesis, Photophysics, and Devices, Inorg. Chem. 46 (2007) 11082-11093.

24 J. N. Demas, G. A. Crosby, Quantum efficiencies of transition-metal complexes. I. d-d Luminescence, J. Am. Chem. Soc. 92 (1970) 7262-7270.

25 Voltamaster 4 software, Radiometer Analytical SAS, Villuerbanne Cedex, France.

26 J. C. de Mello, H. F. Wittmann, R. H. Friend, An Improved Experimental Determination of External Photoluminescence Quantum Efficiency, Adv. Mater. 9 (1997) 230-232.

27 S. B. Heidenhain, Y. Sakamoto, T. Suzuki, A. Miura, H. Fujikawa, T. Mori, S. Tokito, Y. Taga, Perfluorinated Oligo(*p*-Phenylene)s: Efficient n-Type Semiconductors for Organic Light-Emitting Diodes, J. Am. Chem. Soc. 122 (2000) 10240-10241.

28 F. Babudri, D. De Palma, G. M. Farinola, R. Ragni, F. Naso, Synthesis of Functionalized Anthraquinones via Coupling Reactions of 2,6-Diiodo-1,5-dioctyloxy-9,10-anthraquinone, Synthesis 8 (2008) 1227-1232.

29 M. Nonoyama, Benzo[*h*]quinolin-10-yl-*N* Iridium(III) Complexes, Bull. Chem. Soc. Jpn. 47 (1974) 767-768.

30 S. Sprouse, K. A. King, P. J. Spellane, R. J. Watts, Photophysical effects of metal-carbon .sigma. bonds in ortho-metalated complexes of iridium(III) and rhodium(III), J. Am. Chem. Soc. 106 (1984) 6647-6653.

31 D. V. Rosse, Focus on Material Science Research, Nova Science Publishers, 2007.

32 K. Walzer, B. Maennig, M. Pfeiffer, K. Leo, Highly Efficient Organic Devices Based on Electrically Doped Transport Layers, Chem. Rev. 107 (2007) 1233-1271.

33 R. J. Holmes, S. R. Forrest, Y.-J. Tung, R. C. Kwong, J. J. Brown, S. Garon and M. E. Thompson, Blue organic electrophosphorescence using exothermic host–guest energy transfer, Appl. Phys. Lett. 82 (2003) 2422-2424.